

Brazilian Journal of Physics ISSN: 0103-9733 luizno.bjp@gmail.com Sociedade Brasileira de Física Brasil

López-Suspes, Framsol; González, Guillermo A.

Equatorial Circular Orbits of Neutral Test Particles in Weyl Spacetimes
Brazilian Journal of Physics, vol. 44, núm. 4, 2014, pp. 385-397

Sociedade Brasileira de Física

Sâo Paulo, Brasil

Available in: http://www.redalyc.org/articulo.oa?id=46431147012



Complete issue

More information about this article

Journal's homepage in redalyc.org



## PARTICLES AND FIELDS



# **Equatorial Circular Orbits of Neutral Test Particles** in Weyl Spacetimes

Framsol López-Suspes · Guillermo A. González

Received: 4 April 2013 / Published online: 10 June 2014 © Sociedade Brasileira de Física 2014

Abstract A general stability study of equatorial circular orbits in static axially symmetric gravitating systems is presented. We investigate the motion of neutral test particles in circular geodesics such as the marginally stable orbit, the marginally bounded orbit, and the photon orbit are analyzed. We find general expressions for the radius, specific energy, specific angular momentum, and the radius of the marginally stable orbit, both for null and timelike circular geodesics. Different solutions are expressed in different coordinates systems: cylindrical coordinates, oblate spheroidal coordinates, and prolate spheroidal coordinates are considered. We show that all null circular trajectories are unstable, and that there aren't marginally stable null geodesics, whereas for timelike geodesics the motion can be unbounded, bounded, or circular.

**Keywords** Newtonian gravity  $\cdot$  Weyl spacetimes  $\cdot$  Exact solutions  $\cdot$  Equations of motion

#### 1 Introduction

A problem of great importance in the general relativity theory is obtaining the solutions of Einstein's equations. The Einstein field equations or Einstein's equations are a set

F. López-Suspes  $(\boxtimes)$ 

Departamento de Ciencias Básicas, Universidad Santo Tomás Bucaramanga, Colombia

e-mail: framsol@gmail.com

F. López-Suspes · G. A. González Escuela de Física, Universidad Industrial de Santander, A. A. 678, Bucaramanga, Colombia

G. A. González e-mail: guillego@uis.edu.co of ten equations in Einstein's general theory of relativity, which describe the fundamental interaction of gravitation as a result of spacetime being curved by matter and energy. Once the solution is obtained, another important problem is the solution of geodesic equations, whose solutions represent the behavior of test particles that fall freely. The properties of gravitational fields have been studied through of kinematics of test particles, from the point of view of Newtonian gravity [1, 2] and general relativity theory [3]. Since one of the most fundamental characteristics of isolated systems in the universe in a first approximations is axial symmetry, static or stationary axially symmetric exact solutions are of great astrophysical relevance [4]. Consequently, through the years, a great amount of work has been dedicated to theoretical study of this type of exact solutions [5, 6].

Therefore, the solutions of field equations are closely related to the above study, i.e., with the motion analysis of test particles in the gravitational field generated by such distributions of matter. Indeed, the motion study of test particles provides valuable information about the structure and behavior of such gravitational fields. In addition, the study of trajectories in the equatorial plane is of clear astrophysical relevance due to its relation with the dynamics of intergalactic stellar motion or the flow of particles in accretion disks around black holes [4]. In particular, the marginally stable orbit is assumed to roughly represent the inner edge of the accretion disc, the marginally bound orbit bounds the region from where the particles perturbed away from free equatorial circular motion can escape to infinity, and the circular photon trajectory is the limiting orbit below which circular motion is impossible

In the general context, the range of works related to the kinematics of test particles is very large; at present,



the motion of free-falling particles remains a topic of great interest and search in astrophysics, even for the more known and studied solutions, such as the solution of a Schrwarzchild black-hole [8–12] and the Reissner-Nordström solution, which corresponds to the gravitational field of a charged, non-rotating, spherically symmetric body of mass M, [13–15], the exact solution for an uncharged, rotating black hole (Kerr metric) [16–18], the Kerr-Newman black-hole solution (mass, charged, and rotating) [19, 22], and solutions including the cosmological constant [23, 24].

The motion of test particles in axially symmetric spacetimes has been studied by different authors through the years, both for static and stationary spacetimes with different source configurations (see, for instance, references [29] to [33] for Newtonian gravity, and [34] to [45] for general relativity). Now, the purpose of the present work is a general stability study of circular orbits in the equatorial plane in different gravitating systems formed by axially symmetric structures. In particular, we will analyze some important circular geodesics as the marginally stable orbit, the marginally bounded orbit, and the photon orbit. The analysis of the circular trajectory of test particles in the equatorial plane is associated with the study of circular velocity in models of disk galaxies (works of potentialdensity pairs). In turn in these models, the circular velocity is related to the mass density of the galaxy. Specifically in a diagram of circular velocity, the maximum of the curve represents the region where the density of the galaxy is greatest. This is one of the reasons why we are interested in studying the circular orbit, because the radius of the circular orbit defines the separation between the two regions of different densities. For some density-potential pairs of galaxy models in the Newtonian gravity see Ref. [1] for details.

The paper is organized as follows. Section 2 is devoted to deriving the geodesic equations, the *effective potential* and general expressions for the main characteristics of circular orbits: the radius, specific energy, specific angular momentum, and the radius of marginally stable orbit, both for null and timelike geodesics. In the following sections, we particularize these expressions for solutions written in cylindrical coordinates, oblate spheroidal coordinates, and prolate spheroidal coordinates.

In Section 3, we concluded that all null circular orbits are unstable, for solutions expressed in cylindrical coordinates, as illustrated by considering the Chazy–Curzon field. In Section 4, we present the oblate spheroidal coordinates, and some members of the family of Morgan–Morgan disks are analyzed. Later, in Section 5, we consider prolate spheroidal coordinates, and the range of stability of the Erez–Rosen solution is obtained. Finally, results are discussed in Section 6.



The metric for a static axisymmetric spacetime can be written in quasicylindrical coordinates  $(r, \varphi, z)$  as the Weyl line element [5, 6, 46, 47]

$$ds^{2} = -e^{2\Phi}dt^{2} + e^{-2\Phi}[R^{2}d\varphi^{2} + e^{2\Lambda}(d\rho^{2} + dz^{2})], \quad (1)$$

where  $\Phi$ ,  $\Lambda$ , R are functions of  $\rho$  and z only. The ranges of the coordinates  $(\rho, \varphi, z)$  are the standards for cylindrical coordinates (Weyl coordinates) and  $-\infty \le t < \infty$ . The Einstein vacuum equations for this metric are

$$R_{,\rho\rho} + R_{,zz} = 0, (2a)$$

$$(R\Phi_{,\rho})_{,\rho} + (R\Phi_{,z})_{,z} = 0,$$
 (2b)

$$R_{,z}\Lambda_{\rho} + R_{,\rho}\Lambda_{z} - 2R\Lambda_{,\rho}\Phi_{,z} - R_{,\rho z} = 0$$
 (2c)

$$R_{,\rho}\Lambda_{,\rho} - R_{,z}\Lambda_{,z} - R(\Phi_{,\rho}^2 - \Phi_{,z}^2) + R_{,zz} = 0.$$
 (2d)

wherein (), $\alpha = \partial/\partial x^{\alpha}$ . The first equation is the bidimensional Laplace equation for the function R; in order to do, we can consider that R is the real part of the one function  $W(\omega) = R(\rho, z) + iZ(\rho, z)$ . Thus, to find field equations, we consider a transformation [48]

$$\rho \longrightarrow R(\rho, z), \qquad z \longrightarrow Z(\rho, z),$$
 (3)

this is reduced to

$$\Phi \longrightarrow \Phi = \psi, \qquad \Lambda \longrightarrow \gamma = \Lambda - \ln|dW/d\omega|, \qquad (4)$$

here  $W = \omega \pm \alpha \sqrt{\omega^2 - 1}$ , and where  $\alpha$  is a positive constant. Hence, the equation (Eq. 1) becomes [5, 6, 46, 47]

$$ds^{2} = -e^{2\psi}dt^{2} + e^{-2\psi}[\rho^{2}d\varphi^{2} + e^{2\gamma}(d\rho^{2} + dz^{2})], \quad (5)$$

where  $\gamma$  and  $\psi$  are functions of  $\rho$  and z only. The Einstein vacuum equations reduce to the system of Weyl equations [5, 6, 46, 47]

$$\psi_{,\rho\rho} + \frac{1}{\rho}\psi_{,\rho} + \psi_{,zz} = 0,\tag{6}$$

$$\gamma_{,\rho} = \rho \left( \psi_{,\rho}^2 - \psi_{,z}^2 \right),\tag{7}$$

$$\gamma_z = 2\rho \,\psi_{,\rho} \psi_{,z},\tag{8}$$



wherein Eq. (6) is the well-known Laplace's equation (linear differential equation) in cylindrical coordinates with axial symmetry, which is the integrability condition of the overdetermined system Eqs. (7–8). Due to the linearity of Laplace's equation, several authors study the superposition of Weyl fields using the principle of superposition of linear differential equations. The authors superposed two solutions of the function  $\psi$  to obtain one new solution that could represent, e.g., the superposition of one black hole and one thin disk (galaxy) [7]. Nevertheless, in spite of their obvious and simple symmetry properties, the physical interpretation of these solutions is generally far from trivial. For static axisymmetric vacuum solutions, the regularity condition on the axis of symmetry means  $\gamma = 0$  in the limit  $\rho \rightarrow 0$ . If this condition is not satisfied for some value or range of z, then some kind of singularity occurs at these points, see [5, 6].

The solutions of Laplace's equation for the metric function  $\psi$  are similar to the expressions of multipolar expansion of gravitational potential in Newtonian gravity (or in the Euclidean 3-space), but unfortunately the physical meaning of the solutions is not the same in general relativity, e.g., the monopolar term in the multipolar expansion corresponding to gravitational field of a point mass in Newtonian gravity ( $\psi = -Gm/r$ , being m the mass of the source, G the gravitational constant, and r the radial coordinate of spherical coordinates), which is not in general relativity the correct physical interpretation of the spacetimes. In fact, in general relativity, the metric functions do not represent the gravitational potential, although in this case they keep a special similarity through Laplace's equation.

The corresponding Lagrangian for this line element Eq. (5) is given by:

$$2\mathcal{L} = -e^{2\psi}\dot{t}^2 + e^{-2\psi}[\rho^2\dot{\varphi}^2 + e^{2\gamma}(\dot{\rho}^2 + \dot{z}^2)],\tag{9}$$

where the dot represents the derivative with respect to the affine parameter along the geodesic,  $\lambda$ . Now, as the Lagrangian is independent of t and  $\varphi$ ,

$$-E = \partial \mathcal{L}/\partial \dot{t}, \qquad \ell = \partial \mathcal{L}/\partial \dot{\varphi}, \tag{10}$$

are conserved quantities, where  $\ell$  is the specific angular momentum and E is the specific energy with respect to infinity. From the Lagrangian Eq. (9), we can derive the system of equations of motion

$$\ddot{\rho} + (\dot{\rho}^2 - \dot{z}^2)(\gamma_{,\rho} - \psi_{,\rho}) + 2\dot{\rho}\dot{z}(\gamma_{,z} - \psi_{,z}) + e^{-2\gamma} \left[ E^2 \psi_{,\rho} + (\rho \psi_{,\rho} - 1) \frac{\ell^2 e^{4\psi}}{\rho^3} \right] = 0,$$
 (11)

$$\ddot{z} - (\dot{\rho}^2 - \dot{z}^2)(\gamma_{,z} - \psi_{,z}) + 2\dot{\rho}\dot{z}(\gamma_{,\rho} - \psi_{,\rho}) + e^{-2\gamma}\psi_{,z} \left[ E^2 + \frac{\ell^2 e^{4\psi}}{\rho^2} \right] = 0.$$
 (12)

This autonomous system has a unique solution when conditions  $x_0^a = x^a(\lambda_0)$  and  $u_0^a = \dot{x}^a(\lambda_0)$  are given, with  $x^a = \rho$ , z. The initial condition for the velocity of particle can be obtained by using Eq. (10) in the form

$$\dot{t} = Ee^{-2\psi}, \qquad \dot{\varphi} = \ell e^{2\psi}/\rho^2,$$

then our equation Eq. (9) becomes

$$\dot{z}^2 = e^{-2\gamma} \left[ E^2 - e^{2\psi} \left( 2\mathcal{L} + \frac{\ell^2}{\rho^2} e^{2\psi} \right) \right] - \dot{\rho}^2.$$

Therefore, we have only one free parameter  $(\dot{\rho}(0) = \dot{\rho}_0)$ : the initial positions are chosen according to the graph of the effective potential, whereas the initial speed z can be obtained using (2) and including a value of  $\dot{\rho}_0$ .

Now, if we confine the motion of the particle to the equatorial plane z=0, from Eq. (9), we obtain for the radial coordinate  $\rho$ , the equation

$$\dot{\rho}^2 = e^{-2\gamma} \left[ E^2 - e^{2\psi} \epsilon^2 - \frac{\ell^2}{\rho^2} e^{4\psi} \right],\tag{13}$$

with  $\epsilon=1$  for timelike geodesics and  $\epsilon=0$  for null geodesics. The orbit of particle in the equatorial plane can be obtained by solving together the above equation and the equation

$$\dot{\varphi} - \ell e^{2\psi} \rho^{-2} = 0, \tag{14}$$

that follows from Eq. (10). For purely radial motion, we have that  $\varphi = \varphi_0 = constant$ , so that  $\ell = 0$  in the above expressions.

The behavior of trajectories in the equatorial plane is determined by the equation Eq. (9), that can be conveniently expressed as:

$$\frac{\dot{\rho}^2 e^{2\gamma}}{2} + \frac{e^{2\psi}}{2} \left[ \epsilon^2 + \frac{\ell^2}{\rho^2} e^{2\psi} \right] = \frac{E^2}{2},\tag{15}$$

so that we can define an effective potential through the equality

(11) 
$$V(\rho) = e^{2\psi} \left[ \epsilon^2 + \frac{\ell^2}{\rho^2} e^{2\psi} \right],$$
 (16)



which only depends on  $\rho$  and the metric function  $\psi$ . On the other hand, for the metric in Eq. (5) to be asymptotically flat, the functions  $\psi$  and  $\gamma$  must vanish at infinity. So, we can obtain the general condition

$$\lim_{\rho \to \infty} V = \epsilon^2,\tag{17}$$

for all the effective potentials of the form Eq. (16).

Now, for circular orbits, we have that  $\rho = \rho_c = constant$  and so  $\dot{\rho} = \ddot{\rho} = 0$ . Accordingly, from Eq. (15) it follows that

$$E^2 = V(\rho), \tag{18}$$

with  $V(\rho)$  given by Eq. (16). Furthermore, the minima of  $V(\rho)$  correspond to stable circular orbits, whereas the maxima of  $V(\rho)$  correspond to unstable circular orbits. Hence, by computing the derivative of  $V(\rho)$ , we obtain the equation for the critical points of effective potential, which can be written as:

$$\ell^2 e^{2\psi} (2\rho \psi_{,\rho} - 1) + \rho^3 \epsilon^2 \psi_{,\rho} = 0 \tag{19}$$

and, for the case of null circular orbits ( $\epsilon = 0$ ), as [7]

$$2\rho\psi_{,\rho} - 1 = 0. (20)$$

So, the radius of the timelike and null circular orbits are given by the roots of the two previous equations, respectively.

The specific angular momentum  $\ell$  for massive particles in circular orbits can be obtained from Eq. (19), and is given by [7]

$$\ell^2 = \frac{\rho^3 \psi_{,\rho} e^{-2\psi}}{1 - 2\rho \psi_{,\rho}},\tag{21}$$

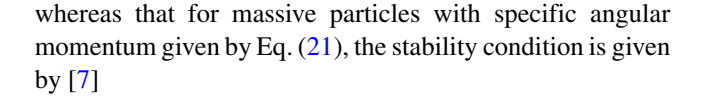
with the condition  $0 \le \rho \psi_{,\rho} < 1/2$ . Accordingly, we can see that the radius of the circular orbits depends on  $\ell$ . Now, by replacing Eq. (21) into Eq. (18), we obtain the other constant of motion, E, for a particle moving in a circular trajectory

$$E^{2} = \frac{e^{2\psi}(1 - \rho\psi_{,\rho})}{(1 - 2\rho\psi_{,\rho})},$$
(22)

where, again,  $0 \le \rho \psi_{,\rho} < 1/2$ .

The stability condition for circular orbits is given by  $V''(\rho_c) > 0$ . Therefore, for massless particles, the stability condition reduces to

$$\psi_{,\rho} + \rho \psi_{,\rho\rho} > 0, \tag{23}$$



$$\rho \psi_{,\rho\rho} + 3\psi_{,\rho} + 2\rho \psi_{,\rho}^{2} (2\rho \psi_{,\rho} - 3) > 0, \tag{24}$$

with  $0 \le \rho \psi_{,\rho} < 1/2$ .

Now, it can be shown that the expressions

$$V''(\rho) = 0 \tag{25}$$

and [7]

$$\frac{d\ell^2}{d\rho} = 0\tag{26}$$

are equivalent for massive particles. Accordingly, the radius of the marginally stable circular orbit can be obtained through the two simultaneous equations  $V'(\rho)=0$  and  $V''(\rho)=0$  or by means of equation  $d\ell^2/d\rho=0$ , provided that there exists two critical points for the *effective potential*, one of them corresponding to the stable circular orbit and the other one to the unstable circular orbit, i.e., according to the criterion of the first derivative, if there is a position where  $d\ell^2/d\rho=0$  (zero slope in the curve  $\ell^2=\ell^2(\rho)$ ), this implies that there is a region where the slope is positive  $d\ell^2/d\rho>0$  (stable region, there is a minimum) and another where  $d\ell^2/d\rho<0$  (unstable region, there is a maximum).

The angular-momentum Eq. (21) is commonly used by several authors in disk-shaped galaxies models to determine the criteria of stability of a fluid at rest in a gravitational field both in Newtonian gravity [1] and in general relativity (see, references [40] to [42]). In this case is known as the Rayleigh criteria [49]. The condition for a stable orbit is

$$\ell \frac{d\ell}{d\rho} > 0.$$

The above expression is fully equivalent to our equation

$$\frac{d\ell^2}{d\rho} \ge 0 \tag{27}$$

where the inequality defines stability of circular orbits to radial perturbations (Rayleigh criteria) and the equality determines the radius of the orbit.

Thus, the minimum value of the specific angular momentum as a function of radius of the circular orbit Eq. (21)



represents the last circular orbit, which is well-known as the marginally stable circular orbit [4, 50]. For null geodesics, the expression is

$$\psi_{,\rho} + \rho \,\psi_{,\rho\rho} = 0,\tag{28}$$

and for timelike geodesic is

$$\rho \psi_{,\rho\rho} + 3\psi_{,\rho} + 2\rho \psi_{,\rho}^{2} (2\rho \psi_{,\rho} - 3) = 0, \tag{29}$$

where  $0 \le \rho \psi_{,\rho} < 1/2$  again. It is important to remark that there are spacetimes that admit more than one marginally stable circular orbit, as well as more than one photon orbit, see reference [7].

It is essential to mention that the equation to determine the stability of photon circular orbit Eq. (23) or the formula to find the radius of marginally stable circular orbit Eq. (28) can be rewritten using the expression Eq. (20) as:

$$\frac{d}{d\rho} \left( \rho \psi_{,\rho} \right) \ge 0 \ . \tag{30}$$

This last expression in accordance with Eq. (20) is always equal to zero, because the function inside the parentheses is constant, and therefore, the derivative with respect to  $\rho$  would always be zero. By the same reasoning, for the inequality (>), a solution cannot be found. In summary, all circular photon orbits are unstable in these solutions. In addition, for the considered Weyl fields, there are no marginally stable circular photon orbits.

Finally, we also find an expression for the angular velocity,

$$\omega = \frac{d\varphi}{dt} = \frac{\dot{\varphi}}{\dot{t}},\tag{31}$$

where  $\dot{t}=E\,e^{-2\,\psi}$  and  $\dot{\varphi}=\ell\,e^{2\,\psi}\,\rho^{-2}$ . For timelike geodesics, we obtain [7]

$$\omega_T^2 = \frac{\ell^2 e^{8\psi}}{E^2 \rho_c^4},\tag{32}$$

where  $\rho_c$  are the roots of Eq. (19), whereas for null geodesics we have [7]

$$\omega_N = \frac{e^{2\psi}}{\rho_0},\tag{33}$$

where the  $\rho_c$  are the solutions of Eq. (20). The above equations only depend on the metric function  $\psi$ , in such a way that the potential  $\gamma$  is not needed for a qualitative analysis of the particle trajectories in Weyl spacetimes. However, the function  $\gamma$  is necessary for solving the differential equations of particle motion.

#### 3 Solutions in Cylindrical Coordinates

In spherical coordinates  $(r, \theta)$ , the asymptotically flat solutions of the equations system Eqs. (6–8) [6] are

$$\psi_k = -\sum_{n=0}^k \frac{C_n \, P_n}{r^{n+1}},\tag{34}$$

$$\gamma_k = -\sum_{l,m=0}^k \frac{C_l C_m (l+1)(m+1)}{(l+m+2)r^{l+m+2}} \times (P_l P_m - P_{l+1} P_{m+1}), \tag{35}$$

wherein  $P_n = P_n(\cos \theta)$  are the usual Legendre polynomials and the  $C_n$  are constants. Now, in the equatorial plane, z = 0, so that we get

$$\psi_k = -\sum_{n=0}^k C_{2n} \frac{P_{2n}(0)}{\rho^{2n+1}},\tag{36}$$

$$\gamma_k = -\sum_{l,m=0}^k \frac{C_{2l}C_{2m}(2l+1)(2m+1)}{(2l+2m+2)\rho^{(l+m)/2+1}} \times (P_{2l}P_{2m} - P_{2l+1}P_{2m+1}).$$
(37)

Where  $(\rho, z)$  are the usual cylindrical coordinates, with

$$\rho = r \sin \theta, \qquad z = r \cos \theta.$$

We can find the radius of a circular null orbit by solving Eq. (20), which in these coordinates reduces to

$$\sum_{n=0}^{k} \frac{2C_{2n}P_{2n}(0)(2n+1)}{\rho^{2n+1}} = 1.$$
 (38)

So we obtain

$$\rho^{2k+1} - \sum_{n=0}^{k} a_{2n} \rho^{2n} = 0, \tag{39}$$

where the constants  $a_{2n}$  are greater than zero, which are related to the constants  $C_{2n}$  and  $P_{2n}(0)$ . This polynomial in  $\rho$  is of odd order and so has, at least one real root. Moreover, since there is only one change in sign, there is a positive root. Accordingly, we can say that there exist null circular orbits. On the other hand, it is easy to see that the stability condition is not satisfied, since

$$\rho \,\psi_{k,\rho\rho} + \psi_{k,\rho} = -\sum_{n=0}^{k} \frac{C_{2n} P_{2n}(0)(2n+1)^2}{\rho^{2n+2}} < 0 \tag{40}$$

and so all the circular orbits are unstable. Finally, we can ask for the existence of a marginally stable circular orbit, which must satisfy  $\rho \psi_{,\rho\rho} + \psi_{,\rho} = 0$ , but we find that there



are no positive roots because the corresponding polynomial no change of sign. Therefore, there is no marginally stable orbit.

Now, in order to illustrate the above considerations, we consider the simplest case of the family Eq. (34), the Chazy–Curzon solution [51, 52],

$$\psi_0 = -\frac{m}{r}, \qquad \gamma_0 = -\frac{m^2 \sin^2 \theta}{2r^2},$$
 (41)

which can be obtained by choosing k=0 and  $C_0=m>0$  in Eq. (34). As it can be seen, although the metric function  $\psi_0$  is spherically symmetric, the full solution Eq. (41) is not. In the equatorial plane, the metric functions reduce to

$$\psi_0 = -\frac{m}{\rho}, \qquad \gamma_0 = -\frac{m^2}{2\rho^2}. \tag{42}$$

This expression is commonly associated to the Newtonian potential of a point mass located at  $\rho=0, z=0$ . However, it can be seen that the resulting spacetimes is not spherically symmetric. Moreover, there is a curvature singularity at  $\rho=0, z=0$  that is not surrounded by a horizon and is therefore naked. Nevertheless, any light emitted from it becomes infinitely red-shifted, so that it is effectively invisible, see [6].

So, according to Eq. (38), for this solution the radius of the unstable circular orbit is  $\rho = 2m$  for photons. Then, with  $\rho = 2m$ , the values of the specific energy and the angular velocity of the particle are

$$\omega_N = (2me)^{-1}, \qquad E_N = \ell \,\omega_N, \tag{43}$$

where  $\ell$  is an arbitrary constant and e is the base of natural logarithms.

In Fig. 1, we show the *effective potential* for lightlike geodesics in the Chazy–Curzon solution. A maximum can be seen at  $\rho=2m$  with a value of  $(2me)^{-2}\ell^2$ . Trajectories are described using the horizontal lines  $(V=E^2)$  to different values of the quantities m and  $\ell$ . When  $0 < E_1 < 1$ 

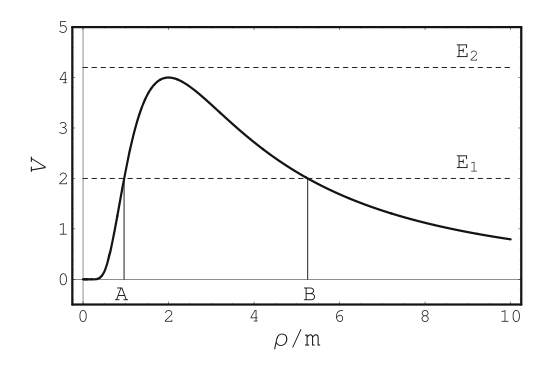


Fig. 1 The *effective potential* for the massless particle in the Chazy–Curzon field. Here, we take  $\ell=4me$ 

 $(2me)^{-2}\ell^2$ , the motion corresponds to a particle with specific energy  $E_1$  coming from infinity until it reaches the turning point B and then goes back to infinity. There is also a potential well, when the motion is confined to  $0 < \rho/m < A$ , and a not allowed region, for  $A < \rho/m < B$ . On the other hand, when the specific energy is greater than  $(2me)^{-2}\ell^2$  as in the horizontal line  $E_2$ , there are no turning points, and the particle moves only in one direction. Now, although we do not consider here solutions with other values of k in Eq. (36), it can be shown that in general all the *effective potentials* behave as depicted in Fig. 1, whenever the condition  $C_{2n}P_{2n}(0) > 0$  be assumed in this family.

On the other hand, for timelike geodesics, the specific energy and specific angular momentum of a particle in a circular orbit are, respectively,

$$\ell^2 = \frac{\rho^2 m \, e^{2m/\rho}}{\rho - 2m}, \qquad E^2 = e^{-2m/\rho}, \tag{44}$$

wherein  $\rho > 2m$ , so that

$$\omega_T^2 = \frac{e^{-4m/\rho}m}{(\rho - 2m)\rho^2}. (45)$$

The radius of the marginally stable circular orbit obtained by solving the equation Eq. (29), and we find the corresponding specific angular momentum by replacing this radius into Eq. (21). For the Chazy–Curzon field, we find

$$\rho = 5.23m, \qquad \ell = 3.52m,$$
(46)

$$E = 0.826, \qquad \omega_T^2 = \frac{0.00525}{m^2},$$
 (47)

for the marginally stable circular orbit.

The graphics of the *effective potential* Eq. (16) for time-like geodesics in the Chazy–Curzon spacetime are presented in Figs. 2 and 3. In Fig. 2, we see that the shape of the

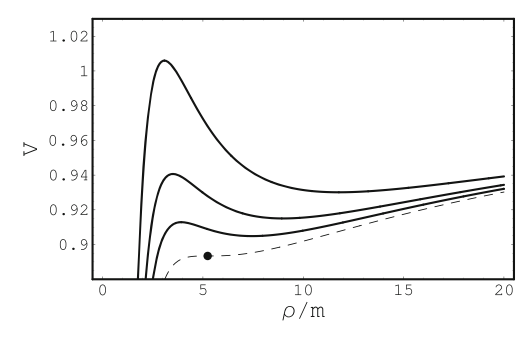


Fig. 2 Effective potential as a function of  $\rho/m$  for timelike geodesics, with different values of  $\ell/m$ , for the Chazy–Curzon field. For the curves from top to bottom, we take  $\ell/m = 4.1, 3.8, 3.65$  and  $\ell = 3.52m$ , respectively. The *point* in the dotted curve corresponds to  $\rho/m = 5.23$ , which is the radius of the marginally stable orbit with  $\ell/m = 3.52$ 



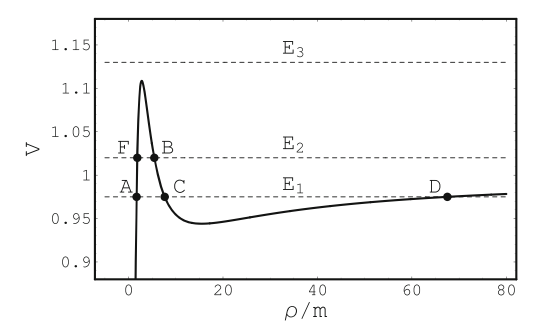
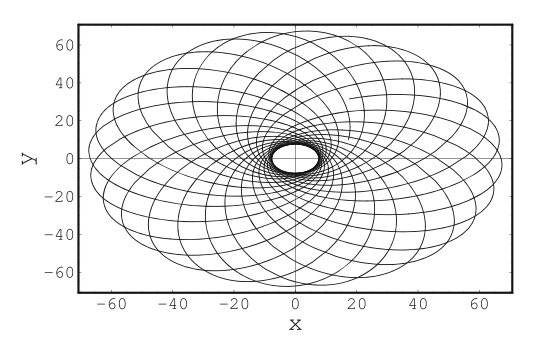
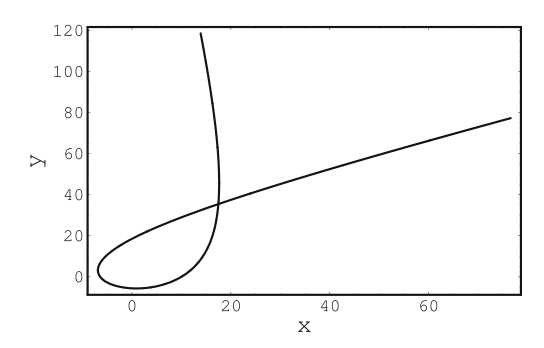


Fig. 3 Effective potential for timelike geodesic with  $\ell=4.5m$  in the Chazy–Curzon spacetimes

effective potential curve depends only on the angular momentum  $\ell$  and that all the curves have two circular orbits, except the doted curve. In this graph, the dotted curve has a value of  $\ell = 3.52m$  and represents the marginally stable circular orbit. Figure 3 shows the potential with  $\ell = 4.5m$ and, with dotted lines, different values of the energy  $E^2$  in order to analyze the possible orbits. Thus, for  $E_1$ , we have three different radiuses as the horizontal line cuts the potential in three points. For the smallest radius A, the particle is confined in the potential well as in Fig. 1,  $0 < \rho/m < A$ . Whereas for the others radius, C and D, we obtain a bounded orbit between them, i.e., if we take  $E_1 = 0.975$ , we find a bounded orbit between  $C = \rho/m \approx 7.66$  (periastron) and  $D = \rho/m \approx 67.52$  (apastron), Fig. 4. When the energy is  $E_2$ , a turning point is found, so for  $E_2 = 1.02$ , the turning point is  $B = \rho/m \approx 5.45$ , and we show in Fig. 5 the corresponding the trajectory. For the point F with energy  $E_2 = 1.02$ , the particle within confined in the potential well, as in A. Whereas for an energy  $E_3$ , greater than the maximum of the potential, there are no turning points and the particle moves only in one direction. Finally, Fig. 6 presents the range of stability for particles moving in a circular orbit by plotting the specific angular momentum, Eq. (44) as a function of the radius of the circular trajectory. The range



**Fig. 4** Orbit of the particle corresponding to the *effective potential* of the Fig. 3 with  $E_1=0.975$ . This orbit is bounded between  $C\approx 7.66$  and  $D\approx 67.52$ . The initial conditions are  $\dot{\rho}(t=0)\approx 0.17$ ,  $\varphi(t=0)=\pi/6$  and  $\rho(t=0)=20$ 



**Fig. 5** Orbit of the particle corresponding to the *effective potential* of the Fig. 3 with  $E_2=1.02$ . The initial conditions used  $\dot{\rho}(t=0)\approx 0.17$ ,  $\varphi=\pi/6$  and  $\rho=20$ 

of stability is  $3.52m \le \ell < \infty$  and  $5.23m \le \rho < \infty$ . The point has coordinates  $(\ell/m, \rho/m) = (3.52, 5.23)$  and corresponds to the radius of the marginally stable circular orbit.

# 4 Solutions in Oblate Spheroidal Coordinates

In the *oblate spheroidal coordinates*, the solution of the Laplace Eq. (6) is

$$\psi_n = -\sum_{k=0}^n C_{2k} P_{2k}(\eta) i^{2k+1} Q_{2k}(i\xi), \tag{48}$$

where  $C_{2k}$  are constants,  $P_k$  are the Legendre polynomials, and  $Q_k$  are the Legendre functions of second kind [53]. This solution represents the exterior Newtonian potential for an infinite family of axially symmetric finite thin disks, recently studied by González and Reina [54], and whose first term, n = 0, is the well-known Kalnajs disk [55]. We also studied in another paper [56] the kinematics around the first four members of this family by means of the Poincaré surfaces of section and Lyapunov characteristic numbers,

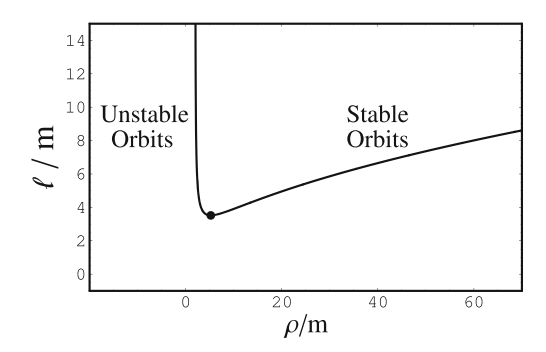


Fig. 6 The specific angular momentum,  $\ell/m$ , as a function of the radius of the circular orbit,  $\rho/m$ , for timelike geodesic in the Chazy–Curzon field. The point has coordinates  $(\ell/m, \rho/m) = (3.52, 5.23)$ . The range of stability is  $3.52m \le \ell < \infty$  and  $5.23m \le \rho < \infty$ 



and found indeed chaos in the case of disk-crossing orbits and completely regular motion in other cases.

The constants  $C_{2k}$  appearing in Eq. (48) are given by:

$$C_{2k} = \frac{mG}{2a} \left[ \frac{\pi^{1/2} (4k+1)(2n+1)!}{2^{2n} (2k+1)(n-k)! \Gamma(n+k+\frac{3}{2}) q_{2k+1}(0)} \right],$$

where  $q_{2k}(\xi) = i^{2k+1}Q_{2k}(i\xi)$ , m is the mass of the disk and G is the gravitational constant. Now, due to the presence of the term (n-k)! at the denominator, all the  $C_{2k}$  constants vanish for k > n. The variables  $\eta$  and  $\xi$  are the oblate coordinates related to the cylindrical coordinates by:

$$\rho^2 = a^2(1 + \xi^2)(1 - \eta^2), \qquad z = a\xi\eta, \tag{49}$$

where a is a constant,  $-1 \le \eta \le 1$  and  $0 \le \xi < \infty$ . In Eq. (49), a is the radius of the thin disk, henceforth, we chose a=1. Studying the circular motion of test particles in disk-like solutions is equivalent to analyzing the behavior of rotation curves in the models of galactic disks. In the plane z=0, there are two regions: if  $\xi=0$  then  $\eta=\sqrt{1-\rho^2}$ , whereas if  $\eta=0$  then  $\xi=\sqrt{\rho^2-1}$ . These two regions correspond to the regions inside and outside of the disk, respectively.

We now write the different equations for these two regions in the simple case of null geodesics. So, from Eq. (20), the radius of the circular orbits inside the source is

$$\sum_{k=1}^{n} 4kC_{2k}q_{2k}(0) \left[ P_{2k-1}(\eta) - \eta P_{2k}(\eta) \right] = \eta, \tag{50}$$

being  $\eta = \sqrt{1 - \rho^2}$ . The stability condition in oblate spheroidal coordinates, inside the disk, take the form

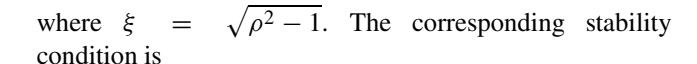
$$\eta(1-\eta^2)\psi_{n,\,\eta\eta} - (1+\eta^2)\psi_{n,\,\eta} \le 0,$$
(51)

that for the solution Eq. (48) can be written as:

$$\sum_{k=1}^{m} 2kq_{2k}(0) \left[ 2k\eta P_{2k}(\eta) + P_{2k-1}(\eta) \right] > 0.$$
 (52)

Now, for null geodesics outside the disk, the radius of the circular orbit can be obtained from the expression

$$\sum_{k=0}^{n} 2C_{2k} P_{2k}(0) \left[ \xi q_{2k}(\xi) + q_{2k+1}(\xi) \right] + \xi = 0, \tag{53}$$



$$\xi(1+\xi^2)\psi_{,\xi\xi} + (\xi^2-1)\psi_{,\xi} \le 0,$$
 (54)

then using Eq. 48 becomes

$$-\sum_{k=0}^{n} C_{2k}(2k+1) \left[ 2\xi q_{2k}(\xi) + q_{2k+1}(\xi) \right] > 0.$$
 (55)

The first solution of Eq. (48), when n = 0, was obtained independently by Zipoy [57] and Vorhees [58], and interpreted by Bonnor and Sackfield [59] as the gravitational field of a pressureless static thin disk, which is singular at the rim. The function  $\psi$  for the first three family members of disks Eq. (48) is given by [54, 56]

$$\psi_{1} = -\mu[\cot^{-1}\xi + A(3\eta^{2} - 1)],$$

$$\psi_{2} = -\mu[\cot^{-1}\xi + \frac{10A}{7}(3\eta^{2} - 1) + B(35\eta^{4} - 30\eta^{2} + 3)],$$

$$\psi_{3} = -\mu[\cot^{-1}\xi + \frac{10A}{6}(3\eta^{2} - 1) + \frac{21B}{11}(35\eta^{4} - 30\eta^{2} + 3)$$

$$(56)$$

(58)

 $+ C(231n^6 - 315n^4 + 105n^2 - 5)$ ].

with

$$A = \frac{1}{4}[(3\xi^2 + 1)\cot^{-1}\xi - 3\xi],$$

$$B = \frac{3}{448}[(35\xi^4 + 30\xi^2 + 3)\cot^{-1}\xi - 35\xi^3 - \frac{55}{3}\xi],$$

$$C = \frac{5}{8448}[(231\xi^6 + 315\xi^4 + 105\xi^2 + 5)\cot^{-1}\xi - 231\xi^5 - 238\xi^3 - \frac{231}{5}\xi],$$

being  $\mu = m/a$ .

For n = 1, the other metric function is [5, 60, 61]

$$\gamma_{1} = 9\mu^{2}(\eta^{2} - 1) \left[ 9\xi^{2}\eta^{2} - \xi^{2} + 4\eta^{2} + 4 + (\xi^{2} + 1)(9\xi^{2}\eta^{2} - \xi^{2} + \eta^{2} - 1)(\cot^{-1}\xi)^{2} - 2\xi(9\xi^{2}\eta^{2} - \xi^{2} + 7\eta^{2} + 1)\cot^{-1}\xi \right] / 16.$$
 (59)



This disk is also singular at the rim [62]. For n = 2, the metric function  $\gamma$  is given by:

$$\gamma_{2} = 25\mu^{2}(\eta^{2} - 1) \left\{ 9\xi^{6} \left( 1225\eta^{6} - 1275\eta^{4} + 315\eta^{2} - 9 \right) \right. \\ \left. + 3\eta^{4} \left( 5050\eta^{6} - 3630\eta^{4} + 366\eta^{2} + 6 \right) \xi^{4} \right. \\ \left. + \left( 4945\eta^{6} - 723 - 45\eta^{2} - 81 \right) \xi^{2} \right. \\ \left. - 6 \left[ 375\eta^{6} + 113\eta^{4} + 15\eta^{2} + 27 \right. \\ \left. + 3 \left( 1225\eta^{6} - 1275\eta^{4} + 315\eta^{2} - 9 \right) \xi^{6} \right. \\ \left. + \left( 6275\eta^{6} - 4905\eta^{4} + 681\eta^{2} - 3 \right) \xi^{4} \right. \\ \left. + \left( 3005\eta^{6} - 1111\eta^{4} - 105\eta^{2} + 3 \right) \xi^{2} \right] \xi \cot^{-1} \xi \right. \\ \left. + 9(\xi^{2} + 1) \left[ 9\eta^{6} + 5\eta^{4} - 5\eta^{2} - 9 \right. \\ \left. + \xi^{6} \left( 1225\eta^{6} - 1275\eta^{4} + 315\eta^{2} - 9 \right) \right. \\ \left. + \xi^{4} \left( 1275\eta^{6} - 785\eta^{4} + 17\eta^{2} + 5 \right) \right. \\ \left. + \xi^{2} (315\eta^{6} - 17\eta^{4} - 47\eta^{2} + 5) \right] (\cot^{-1} \xi)^{2} \right. \\ \left. + 256 \left( \eta^{6} + \eta^{4} + \eta^{2} + 1 \right) \right\} / 2048.$$
 (60)

For  $n \ge 2$ , although the metric function  $\gamma$  can be easily obtained by integrating Eqs. (7–8) properly written in oblate spheroidal coordinates. They are not explicitly presented here due to their highly complex expressions.

Now, we analyze some examples. If we take n=1, the second member of family of disks, we obtain for the radius of circular trajectory, the angular velocity, and specific energy corresponding to this radius, the relations

$$\rho^2 = \frac{2}{3\pi\,\mu}, \qquad \omega_N^2 = \frac{E^2}{\ell^2} = \frac{3\pi\,\mu}{2} \,e^{1-3\pi\,\mu},\tag{61}$$

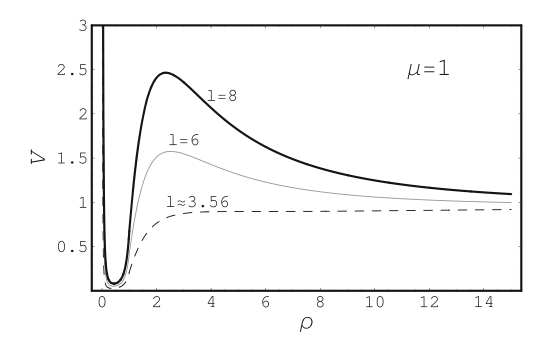


**Fig. 7** *Effective potential* inside and outside of the source for massive particles for the second member of the family of Morgan and Morgan disks, n = 1, with  $\mu = 1$ 

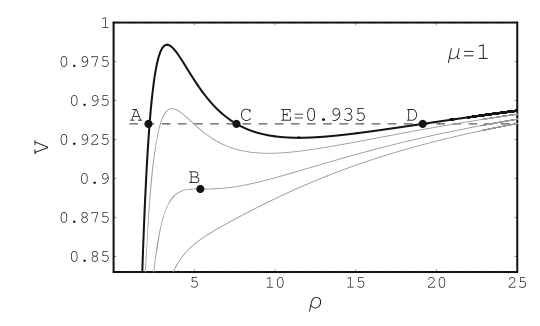


**Fig. 8** *Effective potential* outside of source for the third member of the family of Morgan and Morgan disks, n=2, for a timelike geodesic with  $\mu=1$ 

where  $\mu \geq 2/3\pi$  (due to  $0 \leq \rho \psi_{,\rho} < 1/2$ ),  $\ell$  is an arbitrary constant, and the radius corresponds to a stable equilibrium of the *effective potential* for a null geodesic. Now, outside of the source, the *effective potential* increases until a maximum value, corresponding to the unstable circular orbit, and then diminishes until 0 when  $\rho$  increases, according to Eq. (17). Again, we cannot find the marginally stable circular orbit in this disk for the massless particles.

The behavior of the *effective potential* for different parameter values is similar to those displayed in Fig. 7, corresponding to the timelike geodesic. In the *effective potential* of Fig. 7, we choose  $\ell = 8$ , 6 (gray curve) and 3.56 (dotted curve). The behavior for different parameter values is similar, so we take  $\mu = 1$  as an example. In the exterior case, we consider the third member of the family, n = 2, see Fig. 8. In this graph, the point *B* corresponds to the radius of the marginally stable circular orbit, which has  $\ell \approx 3.688$ . The points *C* and *D* have angular momentum  $\ell = 4.2$  and *effective potential* 0.935, the motion is bounded between the radius 7.61 and 19.14, Fig. 9. In this graph, we choose  $\mu = 1$ .

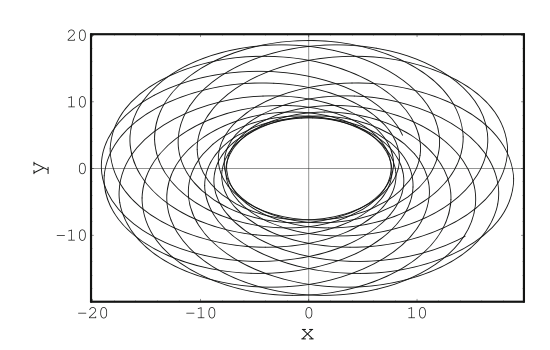


**Fig. 9** Orbit of a particle with E=0.935. The initial conditions are  $\dot{\rho}(0)=0.0903$ ,  $\varphi(0)=\pi/6$ , and  $\rho(0)=10$ . The trajectory is between  $C\leq\rho\leq D$ 



### 5 Solutions in Prolate Spheroidal Coordinates

The general static axisymmetric vacuum solution for  $\psi$  in prolate spheroidal coordinates (u, v) is given by [63]

$$\psi_l = \sum_{n=0}^{l} (-1)^{n+1} d_n Q_n(u) P_n(v), \tag{62}$$

wherein  $u \ge 1$ ,  $-1 \le v \le 1$  and the  $d_n$  are constants related with the multipole moments [63–65].  $P_n$  are the Legendre polynomials and  $Q_n$  are Legendre functions of second kind. These coordinates are related with Weyl's canonical coordinates by:

$$\rho^2 = m^2 (1 - v^2)(u^2 - 1), \qquad z = muv, \tag{63}$$

where m is the mass of the source that produces the field.

The asymptotically flat solution for  $\gamma$  was found by Quevedo [63]. The monopolar solution, l=0, with  $d_0=1$  corresponds to the Schwarzschild spacetimes. The solution of Eq. (20), for the monopolar term, is u=2, that is the unstable radius of a null circular orbit in the Schwarzschild field. For a complete study of motion in Schwarzschild solution in the equatorial plane, see [3]. The solution of Eq. (62) for l=2 is the Erez–Rosen metric [66],

$$\psi_1 = \frac{d_0}{2} \ln \frac{u - 1}{u + 1} + \frac{d_2}{2} (3v^2 - 1) \left[ \frac{1}{4} (3u^2 - 1) \ln \frac{u - 1}{u + 1} + \frac{3}{2} u \right].$$
 (64)

In this case,  $d_0$  and  $d_2$  are related with the monopole and arbitrary quadrupole moment, respectively, [65]. The study of orbits in this solution was developed by different authors [26–28, 34, 35].

Now, in this section, we expose the expressions for the different quantities corresponding to the motion of a particle in a circular orbit in prolate spheroidal coordinates. That is, the specific energy, the angular velocity, and the radius of the marginally stable circular orbit, which are obtained through of the *effective potential* in the equatorial plane,

$$V = e^{2\psi_l} \left( \epsilon^2 + \frac{e^{2\psi_l} \ell^2}{\left(u^2 - 1\right) m^2} \right).$$

We begin with the equations corresponding to null geodesics, when  $\epsilon=0$ . So, the radius of the circular trajectories can be found by

$$2(u^2 - 1)\psi_{l, u} = u, (65)$$



$$\sum_{n=0}^{l} 2d_{2n} P_{2n}(0)(u^2 - 1) Q'_{2n}(u) = u,$$
(66)

with the stability condition

$$u(u^{2} - 1)\psi_{,uu} + (u^{2} + 1)\psi_{,u} \ge 0, (67)$$

from Eq. (62), we get

$$\sum_{n=0}^{l} d_{2n} P_{2n}(0) \left[ (u^2 - 1) Q'_{2n}(u) - 2nu(2n+1) Q_{2n}(u) \right] \ge 0.$$
 (68)

In the above expression, the equal sign corresponds to the equation for the radius of marginally stable circular orbit. Finally, the other formulas are found by means of Eqs. (18) and (33).

Similarly, for the massive particle, we obtain the expressions

$$\ell^2 = \frac{e^{-2\psi} (u^2 - 1)^2 m^2 \psi_{,u}}{u - 2 (u^2 - 1) \psi_{,u}},\tag{69}$$

$$E^{2} = \frac{e^{2\psi} \left[ u - (u^{2} - 1)\psi_{,u} \right]}{u - 2(u^{2} - 1)\psi_{,u}},$$
(70)

where  $u - 2(u^2 - 1)\psi_{,u} > 0$ , in order that the energy per mass unit and the angular momentum per mass aren't imaginary quantities.

The stability condition and the radius of the marginally stable circular orbit can be obtained, as it was done before in the cylindrical or oblate spheroidal coordinates, by solving the system of equations V'(u) = 0 and V''(u) = 0.

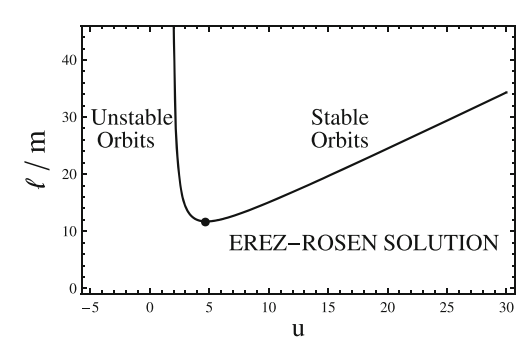


**Fig. 10** Specific angular momentum,  $\ell/m$ , as a function of u for the circular orbit in the Erez–Rosen field with  $d_0 = 1$  and  $d_2 = 1.5$ .



According to this, with the expressions Eqs. (64 and 69), we find

$$\psi_{,u} \left\{ 3u^2 + 2 + 2(u^2 - 1)\psi_{,u} \left[ 2(u^2 - 1)\psi_{,u} - 3u \right] \right\} + u(u^2 - 1)\psi_{,uu} \ge 0,$$
(71)

with 
$$u - 2(u^2 - 1)\psi_{,u} > 0$$
.

Finally, we show in Fig. 10, the region of stability by means of a graph of the specific angular momentum Eq. (69). In particular, we choose  $d_0 = 1$  and  $d_2 = 1.5$  for values of the parameters in the Erez–Rosen solution, it can be seen that the range is

$$0 < u < 4.77,$$
  $4.77 < u < \infty,$ 

and  $11.62 \le \ell < \infty$  for stable orbits. Here, the marginally stable circular orbit has coordinates  $(\ell/m, u) = (11.62, 4.77)$ . In the Newtonian gravity,  $d_2$  usually represents the major deviation from the spherical symmetry, the quadrupolar moment. The case  $d_2 > 0$ , on which we focus here, corresponds to bodies with prolate deformation  $(d_2 < 0)$  represents oblate deformation).

In addition, for spherical coordinates, if we consider deviations from spherical symmetry in these solutions of Weyl family, without perturbing directly the Schwarzschild metric, we must consider the transformation [7]

$$\rho^2 = r(r - 2M)\sin^2\theta, \qquad z = (r - M)\cos\theta, \tag{72}$$

wherein M is the mass of Schwarzschild, and r and  $\theta$  are Schwarzschild coordinates. The simplest type of Weyl solution represents a homogeneous rod of mass M and length 2M placed around the origin (Chazy–Curzon field in cylindrical coordinates). Note that in these coordinates the event horizon is now at  $\rho=0$ . This can be seen from the angular momentum plots in Figs. 6 and 10. The graphs show that as  $\rho$  approaches 0 from the right, the values of  $\ell^2$  increase without bound, i.e., the motion is more chaotic as particle approaches the horizon, as we might have expected from Israel's theorem [67]. This was already mentioned in [68] for gamma spacetime and for M-Q solution in [43].

#### 6 Concluding Remarks

We analyzed the behavior of free-test particles in the equatorial plane of static axisymmetric spacetimes. Different solutions were expressed in different coordinates systems: cylindrical coordinates, oblate spheroidal coordinates, and prolate spheroidal coordinates were considered. We presented several general expressions for the circular orbit in null and

timelike geodesics: radius, specific energy, specific angular momentum, angular, and radius of the marginally stable circular orbit, all of them obtained through an effective potential. The specific angular momentum was presented for the timelike geodesic and was used to find the range of stability of the orbit of the particle, so the minimum value represents the marginally stable circular motion.

In order to obtain the particle trajectory, we analyzed the resulting analytical results. The character of the motion is determined essentially by means of the behavior of effective potential. Thus, we displayed different graphs of effective potential before solving the differential equations of motion of the particle. Then, we began with the Chazy–Curzon field in the case of cylindrical coordinates, as discussed in Section 3. The motion of particles around oblate deformed bodies was developed in Section 4, by means of the analysis of the properties of some member of the family disks Eq. (48). On the other hand, the prolate case was presented in Section 5, where we found the range of stability of the Erez–Rosen solution in the special case of massive particles.

In summary, we concluded that for these solutions all the circular orbits are only unstable in the case of null geodesic, whereas there do not exist marginally stable circular orbits for null godesics. In particular, in cylindrical coordinates, this is fulfilled for the  $C_{2n}P_{2n}(0)>0$  condition. In contrast, we found that for massive particles the orbits can be unbounded, bounded, or circular. This behavior can be seen by means of the *effective potential* and verified by solving the equations of motion numerically. Moreover, for the timelike geodesic, we found the radius of the marginally stable circular orbit in different coordinate systems, cylindrical, prolate, and oblate.

**Acknowledgments** GAG was supported by Vicerrectoria de Investigación y Extensión, Universidad industrial de Santander, through the grant No. 1347 and the grant No. 5705

# References

- J. Biney, S. Tremaine. Galatic Dynamics, Second Edition (Princeton University Press, Pinceton, USA, 2008)
- D. Boccaletti, G. Pucacco. Theory of orbits. Volume 1, Third edition (Springer, 2004)
- M. P. Hobson, G. P. Efstathiou, A. N. Lasenby. General Relativity: an Introduction for Physicists (Cambridge University Press, Cambridge, UK, 2007). Chandrasekhar, S.: The Mathematical Theory of Black Holes. Oxford University Press: New York (1998); Shapiro, S.L. and Teukolsky, S.A.: Black Hole White Dwarfs, and Neutron Stars. John Wyley & Sons, Inc., Weinheim, Germany (1983)
- O. Semerák, T. Zellerin, M. Žáček, The structure of superposed Weyl fields. Mon. Not. R. Astron. Soc. 308, 691 (1999)
- D. Kramer, H. Stephani, E. Herlt, M. Maccallum. Exact Solutions of Einstein's Fields Equations, First Edition (Cambridge University Press, New York, USA, 2000)



6. J. Griffiths, J. Podolský. Exact space-times in Einstein's General Relativity (Cambridge University Press, 2009)

- O. Semerák, M. Žáček, T. Zellerin, Test-particle motion in superposed Weyl fields. Mon. Not. R. Astron. Soc. 308, 705 (1999)
- 8. T. Müller, S. Boblest, Visualizing circular motion around a Schwarzschild black hole. Amer. J. Phy. **79**(1), 63 (2011)
- G. Scharf, Schwarzschild geodesics in terms of elliptic functions and the related red shift. arXiv:1101.1207v2
- A. G. Shah, T. S. Keidl, J. L. Friedman, D. Kim, L. R. Price, Conservative, gravitational self-force for a particle in circular orbit around a Schwarzschild black hole in a radiation gauge. Phys. Rev. D. 83, 064018 (2011)
- G. W. Gibbons, M. Vyska, The application of Weierstrass elliptic functions to Schwarzschild null geodesics. Class. Quantum Grav. 29, 065016 (2012)
- V. J. Bolós, Kinematic relative velocity with respect to stationary observers in Schwarzschild spacetime. J. Geom. Phys. 66, 18 (2013)
- S. Grunau, V. Kagramanova, Geodesics of electrically and magnetically charged test particles in the Reissner-Nordström space-time: analytical solutions. Phys. Rev. D. 83, 044009 (2011)
- D. Pugliese, H. Quevedo, R. Ruffini, Circular motion of neutral test particles in Reissner-Nordström spacetime. Phys. Rev. D. 83(2), 024021 (2011)
- D. Pugliese, H. Quevedo, R. Ruffini, Motion of charged test particles in Reissner-Nordström spacetime. Phys. Rev. D. 83(10), 104052 (2011)
- J. Levin, G. Perez-Giz, A periodic table for black hole orbits. Phys. Rev. D. 77(10), 103005 (2008)
- T. Harada, M. Kimura, Collision of an innermost stable circular orbit particle around a Kerr black hole. Phys. Rev. D. 66, 04661 (2011)
- D. Pugliese, H. Quevedo, R. Ruffini, Equatorial circular motion in Kerr spacetime. Phys. Rev. D. 84, 044030 (2011)
- N. Dadhich, P. P. Kale, Equatorial circular geodesics in the Kerr-Newman geometry. J. Math. Phys. 18(9), 1727 (1976)
- V. I. Dokuchaev, Is there life inside black holes? Class. Quantum Grav. 28, 235015 (2011)
- 21. C. Liu, S. Chen, J. Jing, Collision of two general geodesic particles around a Kerr-Newman black hole. arXiv:1104.3225v1
- D. Pugliese, H. Quevedo, R. Ruffini, Equatorial circular orbits of neutral test particles in the Kerr-Newman spacetime. Phys. Rev. D. 88, 024042 (2013)
- Z. Stuchlík, J. Kovar, Pseudo-Newtonian gravitational potential for Schwarzschild-De sitter space-times. IJMPD. 17(11), 2089– 2105 (2008)
- Z. Stuchlík, J. Schee, Influence of the cosmological constant on the motion of magellanic clouds in the gravitational field of Milky Way. JCAP. 09, 018 (2011)
- J. M. Bardeen, Stability of circular orbits in stationary axisymmetric spacetimes. Ap. J. 161, 103 (1970)
- A. Armenti, A classification of particle motions in the equatorial plane of a gravitational monopole-quadrupole field in Newtonian mechanics and general relativity. Celest. Mech. Dyn. Astron. 6, 383 (1972)
- A. Armenti, On a class of exact geodesics of the erez-rosen metric. Internat. J. Theoret. Phys. 16(11), 813 (1977)
- H. Quevedo, L. Parkes, Geodesics in the Erez-Rosen space-time. Gen. Relativ. Gravit. 21, 1047 (1989)
- A. Saa, Chaos around the superposition of a monopole and a thick disk. Phys. Lett. A. 269(4), 204 (2000)
- E. Guéron, P. S. Letelier, Chaotic motion around prolate deformed bodies. Phys. Rev. E 63(3), 352011 (2001)

- E. Guéron, P. S. Letelier, Chaos in pseudo-Newtonian black holes with halos. Astronom. Astrophys. 368(2), 716 (2001)
- J. Ramos-Caro, J. F. Pedraza, P. S. Letelier, Motion around a monopole + ring system: I. Stability of equatorial circular orbits vs regularity of hree-dimensional Motion. Mon. Not. R. Astron. Soc. 414, 3105 (2011)
- P. S. Letelier, J. F. Ramos-Caro, F. López-Suspes, Chaotic motion in axially symmetric potentials with oblate quadrupole deformation. Phys. Lett. A. 375, 3655 (2011)
- H. Quevedo, L. Parkes, On the geodesics in the Erez-Rosen spacetime. Gen. Relativ. Gravit. 23, 495 (1991)
- K. D. Krori, J. C. Sarmah, A geodesic study of the Erez-Rosen space-time. Gen. Relativ. Gravit. 23, 801 (1991)
- A. Saa, R. Venegeroles, Chaos around the superposition of a black-hole and a thin disk. Phys. Lett. A. 259(3-4), 201 (1999)
- O. Semerák, P. Suková, Free motion around black holes with discs or rings: between integrability and chaos - I. Mon. Not. R. Astron. Soc. 404(2), 545 (2010)
- O. Semerák, P. Suková, Free motion around black holes with discs or rings: between integrability and chaos - II. Mon. Not. R. Astron. Soc. 425(4), 2455 (2012)
- 39. J. Young, G. Menon, A charged Erez-Rosen spacetime and gravitational repulsion. Gen. Relativ. Gravit. 32, 1 (2000)
- E. Guéron, P. S. Letelier, Geodesic chaos around quadrupolar deformed centers of attraction. Phys. Rev. E 66, 046611 (2002)
- P. S. Letelier, Stability of circular orbits of particles moving around black holes surrounded by axially symmetric structures. Phys. Rev. D. 68(10), 104002 (2003)
- L. A. D'Afonseca, P. S. Letelier, S. R. Oliveira, Geodesics around Weyl-Bach's ring solution. Class. Quantum Grav. 22, 3803 (2004)
- L. Herrera, Geodesics in a quash-spherical spacetime: a case of gravitational repulsion. Found. Phys. Lett. 18, 21 (2005)
- F. L. Dubeibe, L. A. Pachón, J. D. Sanabría, Chaotic dynamics around astrophysical objects with nonisotropic stresses. Phys. Rev. D. 75, 023008 (2007)
- W. Han, Revised research about chaotic dynamics in Manko et al. spacetime. Phys. Rev. D. 77, 123007 (2008)
- H. Weyl, Ausbreitung elektromagnetischer Wellen über einem ebenen Leiter. Ann. Physik. 54, 117 (1917)
- 47. H. Weyl, Zur gravitationstheorie. Ann. Physik. 59, 185 (1919)
- 48. G. A. González, P. S. Letelier, Relativistic static thin discs with radial stress support. Class. Quantum Grav. 16, 479 (1999)
- L. D. Landau, E. M. Lifshitz. Fluid Mechanics, 2nd ed. (Pergamon Press, Oxford, 1987). Sec. 27
- K. Watarai, S. Mineshige, Where is a marginally stable last circular orbit in super-critical accretion flow. Publ. Astron. Soc. Japan. 55, 959 (2003)
- 51. J. Chazy, Sur le champ de gravitation de deux masses fixes dans la thorie de la relativit. Bull. Soc. Math. France. **52**, 17 (1924)
- 52. H. E. J. Curzon, Cylindrical solutions of Einstein's gravitation equations. Proc. London Math. Soc. 23, 477 (1924)
- 53. H. Bateman. Partial Differential Equations of Mathematical Physics (Cambridge U.P., 1932)
- G. A. González, J. I. Reina, An infinite family of generalized Kalnajs discs. Mon. Not. R. Astron. Soc. 371, 1873 (2006)
- A. J. Kalnajs, The equilibria and oscillations of a family of uniformly rotating stellar disks. Ap. J. 175, 63 (1972)
- J. F. Ramos-Caro, G. A. González, F. López-Suspes, Chaotic and regular motion around generalized Kalnajs discs. Mon. Not. R. Astron. Soc. 386, 440 (2008)
- D. M. Zipoy, Topology of some spheroidal metrics. J. Math. Phys. 7, 1137 (1966)



- B. H. Vorhees, Static axially symmetric gravitational fields. Phys. Rev. D. 2, 2119 (1970)
- W. A. Bonnor, A. Sackfield, The interpretentation of some spheroidal metrics. Commun. Math. Phys. 8, 338 (1968)
- T. Morgan, L. Morgan, The gravitational field of a disk. Phys. Rev. 183, 1097 (1969)
- 61. L. Morgan, T. Morgan, Gravitational field of shells and disks in eneral relativity. Phys. Rev. 2, 2756 (1970)
- O. Semerák, Curvature singularity around first Morgan-Morgan disc. Class. Quantum Grav. 17, 3589 (2001)
- 63. H. Quevedo, Class of stationary axisymmetric solutions of Einstein's equations in empty space. Phys. Rev. **33**(2), 324 (1986)
- H. Quevedo, General static axisymmetric solution of Einstein's vacuum field equations in prolate spheroidal coordinates. Phys. Rev. D. 39, 2904 (1989)
- V. S. Manko, On the description of the external field of a static deformed mass. Class. Quantum Grav. 7(9), L209 (1990)
- 66. G. Erez, N. Rosen, The gravitational field of a particle possessing a multipole moment. Bull. Res. Counc. Isr. **8F**, 47 (1959)
- 67. W. Israel, Event horizons in static vacuum space-times. Phys. Rev. **164**, 1776 (1967)
- 68. L. Herrera, F. Paiva, N. O. Santos, Geodesics in the  $\gamma$  space. Int. J. Modern Phys. D. **9**, 649 (2000)

